JMEPEG (2018) 27:483–491
DOI: 10.1007/s11665-017-2920-3

1059-9495/$19.00

Effect of Holding Pressure on Microstructure and Mechanical Properties of A356 Aluminum Alloy

Xiaoyan Wu, Huarui Zhang, Zhen Ma, Lina Jia, and Hu Zhang

(Submitted May 9, 2017; in revised form July 9, 2017; published online January 22, 2018)

In this study, the effect of holding pressure on microstructure and mechanical properties of low-pressure die cast A356 aluminum alloy was investigated. The results showed that the application of high holding pressure (300 kPa) generated castings with denser structure and superior mechanical properties. By increasing the holding pressure up to 300 kPa, the size of secondary dendrite arm spacing greatly reduced by 22.7% at the cooling rate of 1°C/s and decreased by 12.8% at 10°C/s. The Feret's diameter and aspect ratio of eutectic silicon particles decreased by 8.4 and 5.1% at the cooling rate of 1°C/s and decreased by 9.3 and 6.4% at 10°C/s, respectively. Meanwhile, the density of A356 aluminum alloy increased to 2.678 g/cm^3 and the area fraction of porosity decreased to 0.035%. Thus, tensile properties of A356 aluminum alloy obtained at high holding pressure were enhanced, especially the ductility. All these could be associated with the better filling capability and faster cooling rate caused by high holding pressure. In the analytical range of experimental conditions, the correlation of mechanical properties with process parameters was established by statistical models to predict the ultimate tensile strength and elongation of low-pressure die cast A356 aluminum alloy.

Keywords aluminum, high holding pressure, low-pressure die cast, mechanical, mechanical properties, microstructure

1. Introduction

Nowadays, the increasing demand for weight reduction in automotive industry has resulted in a large research interest in aluminum alloys. Among all the aluminum alloys, A356 aluminum alloy is a good candidate in automotive field due to its good castability, high corrosion resistance and other desirable properties (Ref 1-5). However, the coarse primary α-Al dendrites, acicular-shaped eutectic Si particles and existence of large amount of porosity defects will lower its mechanical properties and limit its industry application. Therefore, the controlling of microstructure is of high order of importance for A356 aluminum alloy.

To date, much attention has been paid to the microstructural controlling technology for A356 aluminum alloy. Traditionally, addition of grain refiner and modificator, such as Al-Ti-B (Ref 6) and Al-Sr (Ref 7) master alloys, is the preferred methods to reduce grain size and modify eutectic silicon particles. To improve the mechanical properties of A356 aluminum alloy further, some new kinds of grain refiners, such as Al-RE (Ref 8), Al-Nb-B (Ref 9, 10) and Al-Sc-Zr (Ref 11), and mechanical or electromagnetic agitation have been introduced into the metallurgical process (Ref 12). In addition, some efforts have also been made to minimize porosity defects (Ref 13, 14). However, all these above methods have single effect which is limited to refine the grain size, or modify the eutectic silicon particles, or minimize the porosity defects. Moreover, the high cost and complexity of the required equipment of above methods preclude their wide use in industry. Therefore, it is essential to develop a method that can improve the microstructures (secondary dendrite arm spacing, eutectic silicon particles and porosity defects) simultaneously.

It is well known that low-pressure die casting (LPDC) technique is the preferred foundry technology for the production of A356 components (Ref 15). Solidification under pressure, which is called holding pressure, is the feature of LPDC process. The main effect of holding pressure is to feed and transport further molten metals into the liquid–solid two-phase region and solid skeleton gap. As was reported by Giulio Timelli et al. (Ref 16), holding pressure from 35 kPa to 50 kPa could refine the secondary dendrite arm spacing (SDAS) and minimize castings porosity level of LPDC A356 aluminum alloy for engine blocks, which decreased from 0.3 to 0.1% and 67 to 58 μm, respectively. Therefore, application of high holding pressure is an effective method that could improve microstructure. Unfortunately, due to the limitation of low-pressure die cast technique and instruments, the holding pressure is generally less than 100 kPa, which has limited effect in improving the microstructure and mechanical properties.

Recently, the authors have developed the LPDC technique and instruments which could improve the holding pressure from 0 to 400 kPa (Ref 17). The existing research results suggest that high holding pressure can increase the mechanical properties by 10-30% for strength and 200-400% for elongation. However, the mechanism for this improvement is still unclear. The main objective of this study is focused on the relationship among the holding pressure, the size of SDAS, the

Xiaoyan Wu, Huarui Zhang, Zhen Ma, Lina Jia, and **Hu Zhang**, School of Materials Science and Engineering, Beihang University, No 37 Xueyuan Road, Beijing 100191, China; and Beijing Key Laboratory for Advanced Functional Material and Thin Film Technology, Beihang University, No 37 Xueyuan Road, Beijing 100191, China. Contact e-mails: wuxiaoyan@buaa.edu.cn, huarui@buaa.edu.cn, mazhen@buaa.edu.cn, jialina@buaa.edu.cn, and zhanghu@buaa.edu.cn.

size of eutectic silicon particles, the amount of microporosity and the mechanical properties of A356 aluminum alloy. Additionally, Weibull statistics method is employed to quantify the effects of different holding pressures on the mechanical properties (UTS and El%) and reliability of castings.

2. Experimental

2.1 Materials and Casting Process

In the present work, A356 aluminum alloy (AlSi7Mg0.3) was supplied as base alloy and its chemical composition is shown in Table 1. The schematic diagram of LPDC machine used in the present study is shown in Fig. 1(a). The structure of analytical component was in the form of an automobile wheel (diameter: 17 in., 6 spokes) as is shown in Fig. 1(b).

The molten aluminum alloy was degassed by injecting N_2 into the pool and carefully skimmed to remove oxides and inclusions from surface of the melt. The liquid metal was then transferred to a holding furnace inside a LPDC unit and held at 700°C. Die casting parameters including filling pressure and filling time at different stages are shown in Fig. 2. During the casting process, the cooling rate was about 1°C/s for spoke and 10°C/s for outer rim which was obtained based on Eq 1. Therefore, independent variables in the present study are summarized in Table 2.

$$\lambda_2 = 39.4R^{-0.317} \quad \text{(Eq 1)}$$

where λ_2 represents the size of SDAS and R represents the mean cooling rate of the primary α-Al dendrites during solidification.

After casting, the wheels were heat-treated according to T6 condition using the following schedule:

Solution treated at 540 ± 5°C for 280 min in an air circulating furnace;
Water quenched at 80°C;
Artificially aged at 154 ± 4°C for 160 min.

Then, the T6 heat-treated A356 aluminum alloy was used to further test and analyze.

2.2 Metallographic Characterization

Schematic of sampling locations for tensile test specimens is shown in Fig. 1. A total of 20 specimens were prepared for each condition. The specimens were machined with the gauge length of 30 mm and cross section diameter of 6 mm. Tensile tests were carried out at room temperature on the Instron Model 8801 testing machine using 1 mm/min strain rate. In this work, two-parameter Weibull distribution (Ref 18) was used to characterize the dispersion of mechanical properties and determine the reproducibility of properties.

Samples for microstructures characterization were taken from the end of corresponding tensile specimens. They were ground using grinding paper ranging from 800 to 3000 grit and polished with 1.5-μm alumina. Subsequently, the samples were ultrasonically cleaned and etched using a reagent containing 5 ml HF and 95 ml distilled water. The optical microscope (Leica DM4000) was used to measure microstructures. The size of SDAS, eutectic silicon particles and porosity were measured using Image Pro Plus metallographic analysis software. The density of specimen was measured based on Archimedes method, and the equation is shown as follows.

$$\rho = \frac{w_1 \rho_w}{w_1 - w_2} \quad \text{(Eq 2)}$$

where ρ is the density of specimen, w_1 is the weight of specimen in the atmosphere, w_2 is the weight of specimen in the water, and ρ_w is the density of water.

3. Results

3.1 Microstructure Characterization

Representative optical microstructures of A356 aluminum alloy obtained from different experimental conditions are shown in Fig. 3. The microstructure of A356 aluminum alloy mainly consisted of primary α-Al solid solution and eutectic mixture of aluminum and silicon. α-Al precipitated from the liquid as the primary phase in the form of dendrites. Porosity defects (marked with red arrows) distributed among the dendrites are presented in Fig. 3. The optical microstructures of the eutectic zone are provided in Fig. 4, which can demonstrate a substantial microstructure difference in size and shape of eutectic silicon particles. The characterization of microstructure was carried out by measuring the size of SDAS and eutectic silicon particles and density. The results are presented in Table 3.

It was observed that when the cooling rates were 1 and 10°C/s, the size of SDAS decreased from 50.68 and 24.85 to 39.2 and 21.66 μm, respectively, with the holding pressure increasing from 85 to 300 kPa. The Feret's diameter and aspect ratio of eutectic silicon particles also decreased. The size distribution of the eutectic silicon particles was investigated, and the results are shown in Fig. 5. The Feret's diameter and aspect ratio of eutectic silicon particles found to follow similar lognormal distributions. By increasing the holding pressure, the distribution of the size of eutectic silicon particles became more centerized. The equivalent Feret's diameter and aspect ratio of eutectic silicon particles with the maximum frequency shifted to lower values, and the absolute value of the maximum frequency increased. The average Feret's diameter of eutectic silicon particles decreased by 8.4% at the cooling rate of 1°C/s and 9.3% at 10°C/s with the increment of holding pressure from 85 to 300 kPa. The aspect ratio decreased by 5.1 and 6.4% correspondingly. Therefore, by increasing the holding pressure, the microstructure was characterized by finer dendrites and eutectic silicon particles.

Table 1 The chemical composition of A356 aluminum alloy

	Si	Mg	Ti	Sr	Fe	Mn	Cu	Sn	Al
Wt.%	6.91	0.297	0.117	0.017	0.144	0.002	0.0009	0.0027	Balance

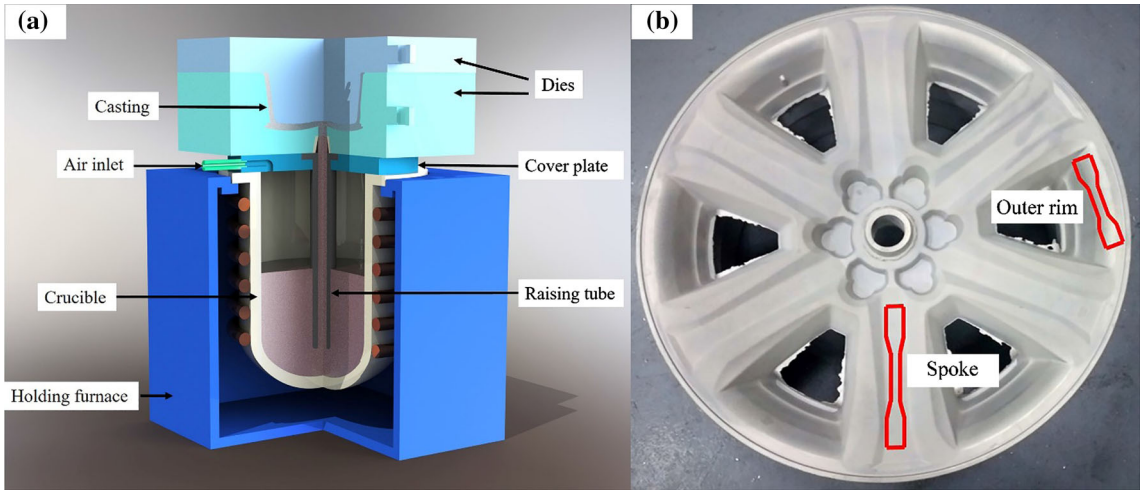

Fig. 1 (a) Schematic diagram of low-pressure die casting machine; (b) schematic diagram for specimen preparation in section spoke and outer rim of automotive wheel

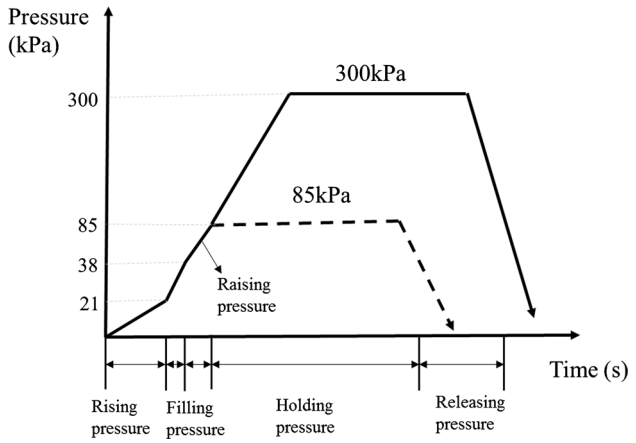

Fig. 2 Parameters of the pressure–time curves of LPDC process

The density of castings reached to the optimal value (2.678 g/cm^3) at the condition of 300 kPa and 10°C/s, which was in good agreement with the optical microstructure in Fig. 3. Porosity defect was a leading cause in the reduction of mechanical properties, particularly ductility. It has been reported by Caceres et al. (Ref 19) that the dominant parameter was the area fraction of defects in the surface that affected the mechanical properties. Therefore, to assess the efficiency of holding pressure, the area fraction of porosity was measured in the analytical region of samples and corresponding result is presented in Fig. 6. It can be summarized from Fig. 6 that the porosity area fraction of specimens solidified at the condition of 85 kPa was in the range from 0.15 to 0.33%. The specimens obtained with higher pressure (300 kPa) showed a porosity level between 0.03 and 0.13%. Therefore, higher holding pressure generated A356 aluminum alloy with lower porosity area fraction and denser structure.

3.2 Tensile Properties

Table 4 shows the tensile test results obtained from every experimental condition. As can be seen, maximum values of tensile properties (UTS and El) corresponded to the specimen obtained with higher holding pressure (300 kPa) and faster cooling rate (10°C/s). At the cooling rate of 1°C/s, average values of UTS and El% increased by 15.1 and 225%, respectively, with the increasing holding pressure. At a cooling rate of 10°C/s, the values of UTS and El% increased by 13.1 and 90.1%, respectively. Therefore, holding pressure was an important factor that influences the tensile properties of LPDC A356 aluminum alloy.

Table 2 Low-pressure die casting parameters varied in this study

Designation	Position	Cooling rate/°C/s	Holding pressure/kPa
LL	A	1	85
LH			300
HL	B	10	85
HH			300

Figure 7 and 8 present the distribution of the tensile test data obtained for the test specimens. It can be seen that the distribution of the data obtained from tensile test looked like to be normal. However, this single analysis was not enough to reveal the effects of different parameters completely. Weibull distribution was used to evaluate the reliability of the mechanical properties in the present study.

3.3 Weibull Analysis

Figure 9 and 10 show the Weibull plots of UTS and El% data obtained from the tensile test specimens. The corresponding linear fit and adjusted R^2 values are also presented in these figures. In the present study, the values of regression coefficients (R^2) for UTS ($R^2_{\mathrm{UTS}} > 0.9$) and El ($R^2_{\mathrm{El}} > 0.95$) in both experiments were greater than the calculated value for $R^2_{0.05}$ which was 0.89378. Therefore, Weibull analysis in the present study was reliable.

$$R^2_{0.05} = 1.0637 - {}^{0.4174}/_{N^{0.3}} \quad \text{(Eq 3)}$$

Table 5 summarizes the results of Weibull analysis for both UTS and El% data for all experiments. Independent of the cooling rate, the Weibull module for high holding pressure

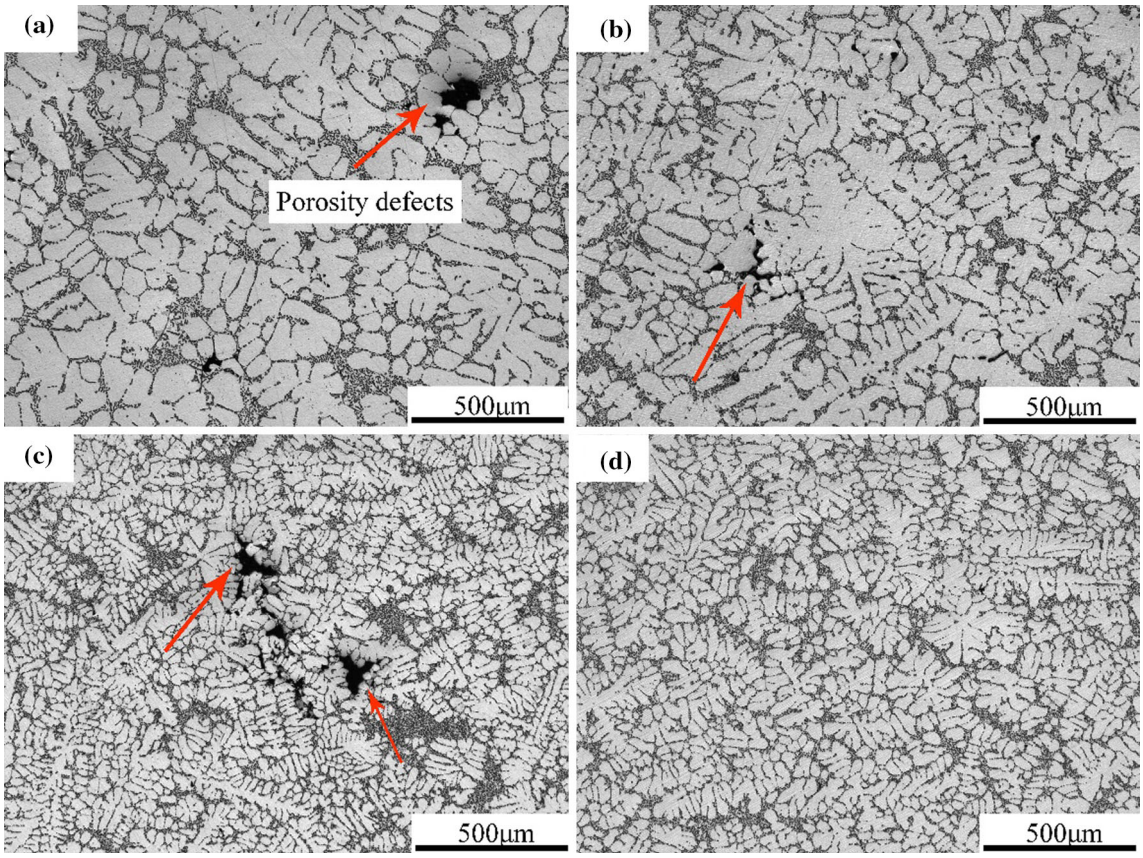

Fig. 3 Typical optical microstructures of LPDC A356 alloy cast under different conditions: (a) 1°C/s, 85 kPa; (b) 1°C/s, 300 kPa; (c) 10°C/s, 85 kPa; and (d) 10°C/s, 300 kPa

(300 kPa) was greater than that for low holding pressure (85 kPa), which suggested that the increment of holding pressure improved the data stability of UTS and El% for LPDC A356 aluminum alloy. The optimal Weibull module value was obtained at the condition of 300 kPa and 10°C/s. All these results indicated that less porosity defects existed in the specimens manufactured with higher holding pressure.

4. Discussion

4.1 Effects of Holding Pressure on SDAS and Eutectic Silicon Particles

With the application of high holding pressure of 300 kPa, the size of SDAS greatly reduced by 22.7% at the cooling rate of 1°C/s and decreased by 12.8% at 10°C/s. The Feret's diameter of eutectic silicon particles decreased by 8.4% at the cooling rate of 1°C/s and decreased by 9.3% at 10°C/s, respectively. It is suggested that high holding pressure can refine the structure of dendrites and eutectic silicon particles. Meanwhile, the aspect ratio of silicon particles also decreased from 1.58 to 1.32, indicating that high holding pressure was beneficial to modification. The refinement of SDAS and eutectic silicon particles was related to the faster cooling rate caused by high holding pressure. The holding pressure of 300 kPa was sufficient to ensure good contact between the casting surface and mold cavity walls, which enhanced the heat transfer and accelerated a significant increase in the cooling rate. According to well-known empirical Eq 1 given in section 2.1, SDAS was inversely proportional to cooling rate. Therefore, SDAS was refined under high holding pressure.

It has been reported in reference (Ref 4) that eutectic temperature decreased with the increase in cooling rate. Therefore, larger regression of eutectic arrest temperature was obtained under high holding pressure and better modification effect was obtained.

4.2 Effects of Holding Pressure on Porosity Defects

It was prone to generate pore and shrinkage porosity defects during solidification process if the holding pressure was inadequate (Ref 16). Based on the growth of gas pore by diffusion, Stefanescu (Ref 20) developed a model for gas pore growth at the end of solidification of casting alloys, which was:

$$P_G + P_{shr} = P_{appl} + P_{st} + P_{exp} + P_r \quad \text{(Eq 4)}$$

where P_G is the pressure exerted by gas evolution, P_{shr} is the negative pressure from resistance to shrinkage-induced flow through the fixed dendrite network, P_{appl} is the applied holding pressure, P_{st} is the metallostatic pressure, P_{exp} is the expansion pressure because of phase transformation, and P_r is the surface tension on the pore. The surface tension P_r was governed by

$$P_r = {}^{2\gamma}/_{r_p} \quad \text{(Eq 5)}$$

where γ is the surface tension and r_p is the pore radius. Therefore, the pore size can be calculated as follows:

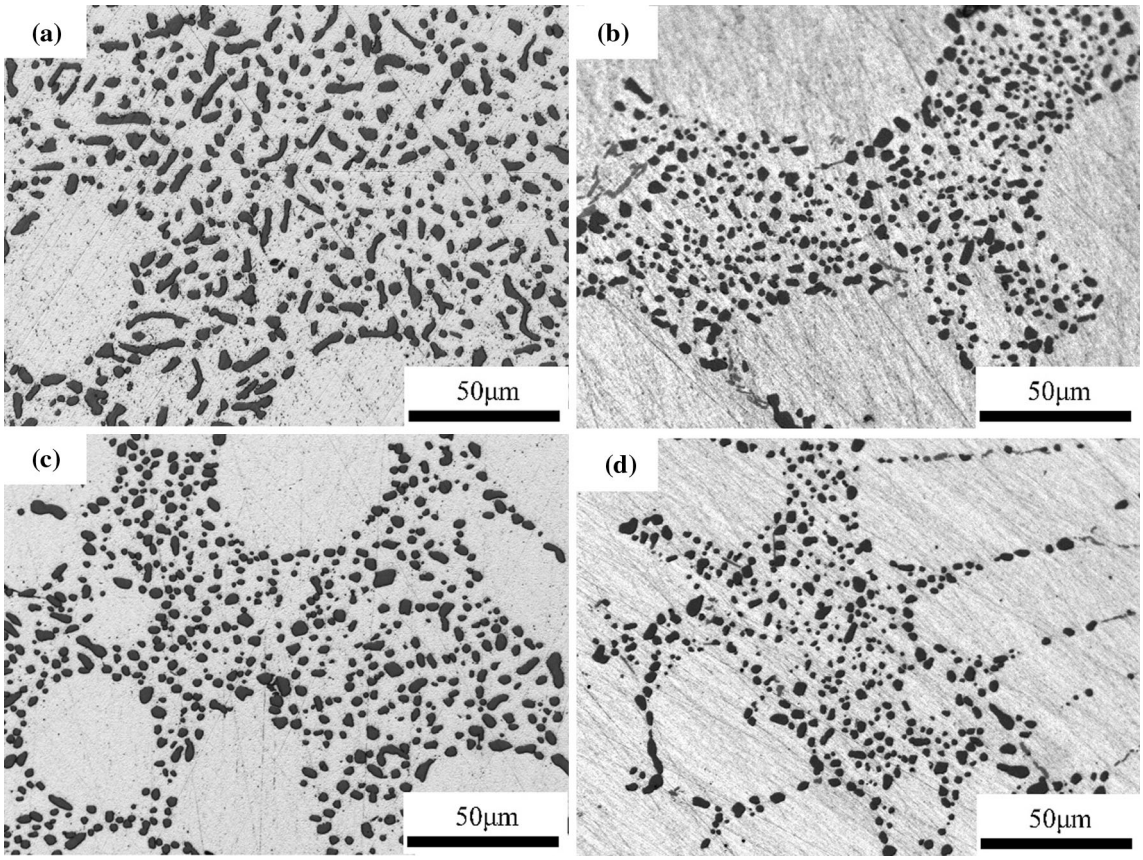

Fig. 4 Silicon crystals in the eutectic regions obtained at (a) 1°C/s, 85 kPa; (b) 1°C/s, 300 kPa; (c) 10°C/s, 85 kPa; and (d) 10°C/s, 300 kPa

Table 3 Results of image analysis

Designation	LL	LH	HL	HH
SDAS (μm)	50.68 ± 3.51	39.2 ± 5.5	24.85 ± 2.93	21.66 ± 2.43
Feret's diameter of Si (μm)	3.2 ± 1.24	2.93 ± 0.93	2.89 ± 0.98	2.62 ± 1.05
Aspect ratio of Si	1.58 ± 0.49	1.5 ± 0.45	1.41 ± 0.31	1.32 ± 0.34
Density (g/cm^3)	2.656	2.667	2.664	2.678

$$r_p = \frac{2\gamma}{P_G + P_{shr} - (P_{appl} + P_{st} + P_{exp})} \quad \text{(Eq 6)}$$

According to the formula, it was evident that the size of porosity can be prevented by increasing the applied holding pressure.

In addition, the criterion of the shrinkage porosity was expressed as follows (Ref 21):

$$G_{sc}\sqrt{P_{sc}}/\sqrt{R_{sc}} < K_c \quad \text{(Eq 7)}$$

where G_{sc}, P_{sc} and R_{sc} are temperature gradient, pressure and cooling rate of the critical solid fraction, respectively, and K_c is the criterion. Therefore, independent of the G_{sc} and R_{sc}, P_{sc} is the key factor to affect the shrinkage porosity defects. According to the above formula, the shrinkage porosity can be minimized or eliminated by increasing holding pressure to improve the solid fraction, which meant that by increasing the holding pressure, the filling capability of the molten metal between dendrite arms was greatly improved. Therefore, with the application of higher holding pressure, the size and amount of gas porosity and shrinkage porosity were minimized in A356 aluminum alloy.

4.3 Effect of Variables on Mechanical Properties

As stated in section 3.2, the increment of holding pressure increased the UTS and elongation. There was no doubt that the superior mechanical properties were related to finer microstructural features as stated in the above sections. An analysis of variance was a statistical methodology that enabled to investigate and model the relationship between the output (UTS and El) and input variables (cooling rate and holding pressure). Tables 6 and 7 summarize the results of analysis of variances for UTS and elongation. The p values were 0.0092 and 0.012 for elongation and 0.0073 and 0.005 for UTS, which were highly below 0.05 for both the features analyzed. Consequently, the effect of relationships between the factors of holding pressure and cooling rate with mechanical properties appeared statistically significant. On the basis of the significance level

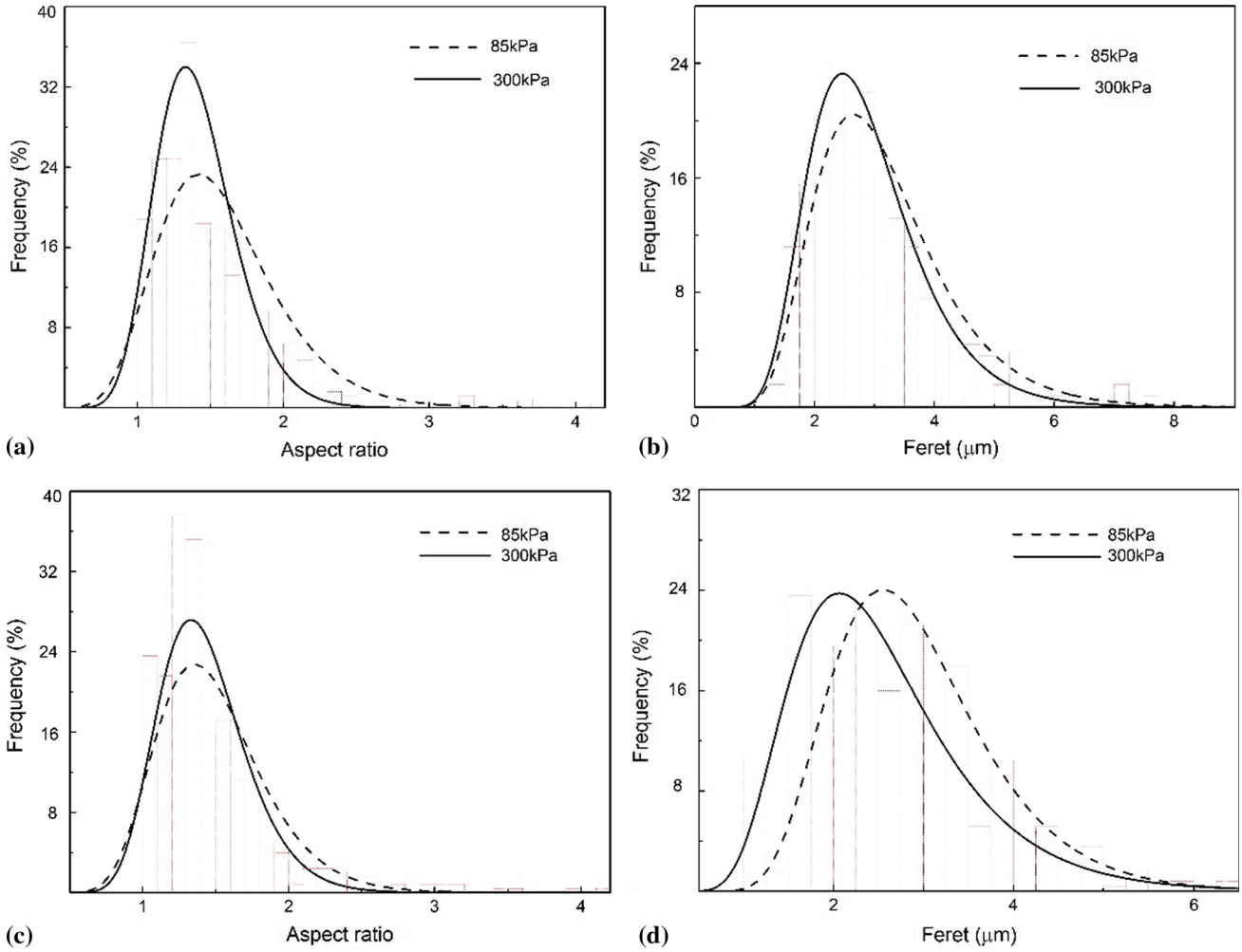

Fig. 5 Distribution of equivalent diameter and aspect ratio for eutectic Si particles estimated as a function of the holding pressures under different cooling rates: (a), (b) 1°C/s; (c), (d) 10°C/s

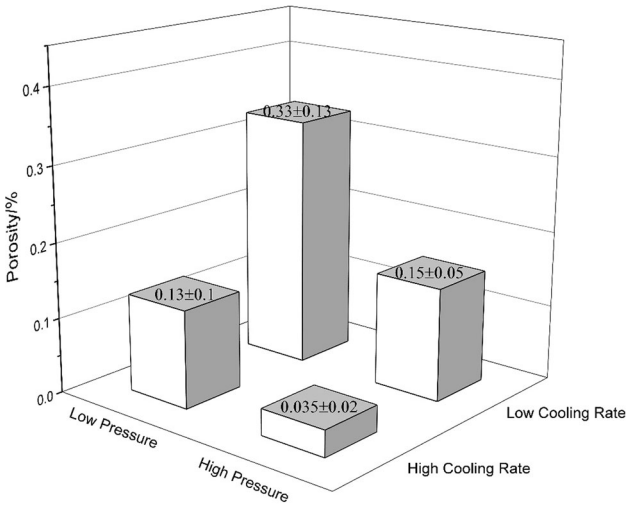

Fig. 6 Influence of holding pressure and cooling rate on the porosity in the analyzed region

provided by the analysis of variance, a linear regression model can be developed describing the relationship between the response (UTS and elongation) and the predictor variables

Table 4 Results of tensile properties under different conditions

Designation	UTS/MPa	E/%
LL	232 ± 10	2.8 ± 0.5
LH	267 ± 6	9.1 ± 0.6
HL	259 ± 5	7.1 ± 0.9
HH	293 ± 11	13.5 ± 1.2

(holding pressure and cooling rate). In the considered range of experimental conditions, the dependent variables (UTS and El) can be described by the following semi-empirical equations:

$$\text{UTS (MPa)} = 215.67 + 2.94 \times (\text{Cooling rate}) + 160.47 \times (\text{Holding pressure}) \quad \text{(Eq 8)}$$

$$\text{El}(\%) = -0.22 + 0.48 \times (\text{Cooling rate}) + 29.53 \times (\text{Holding pressure}) \quad \text{(Eq 9)}$$

where Cooling rate is in °C/s; Holding pressure is in MPa.

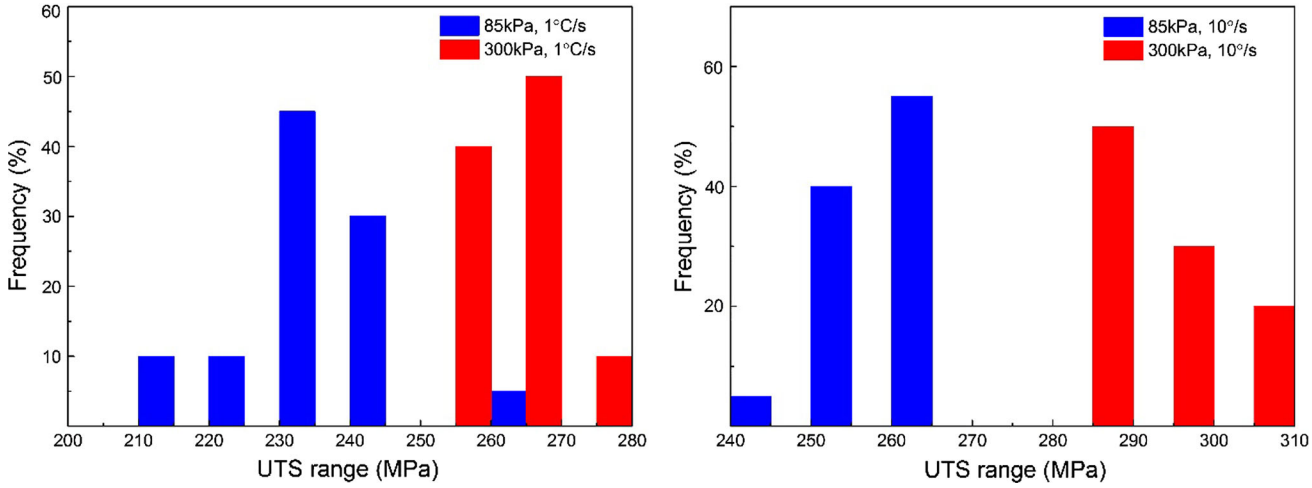

Fig. 7 Frequency plots of ultimate tensile strength (UTS)

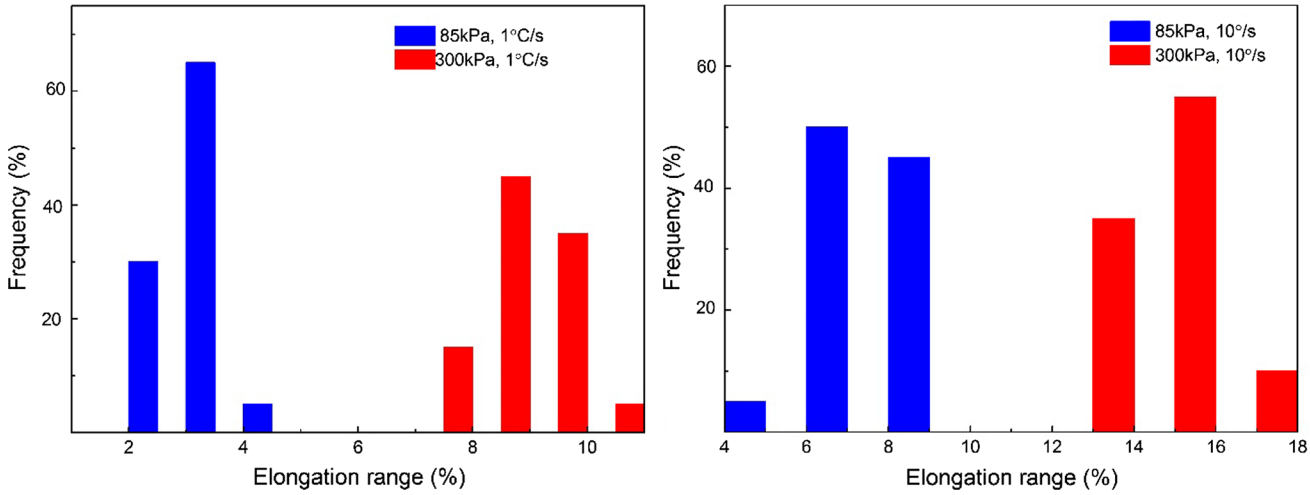

Fig. 8 Frequency plots of elongation

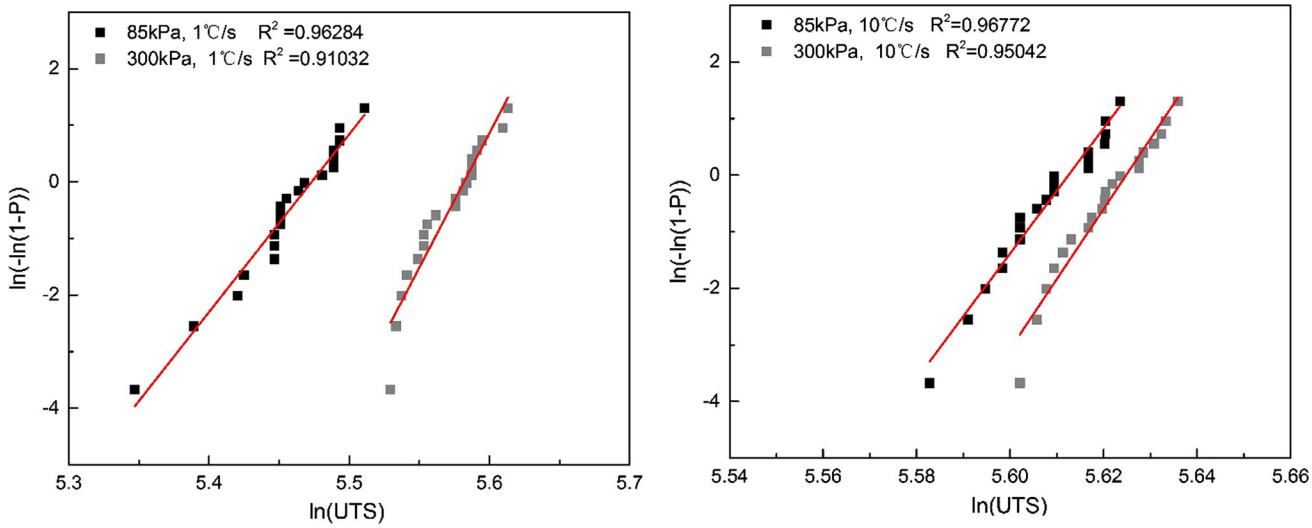

Fig. 9 Weibull plots of UTS data obtained from different experimental conditions

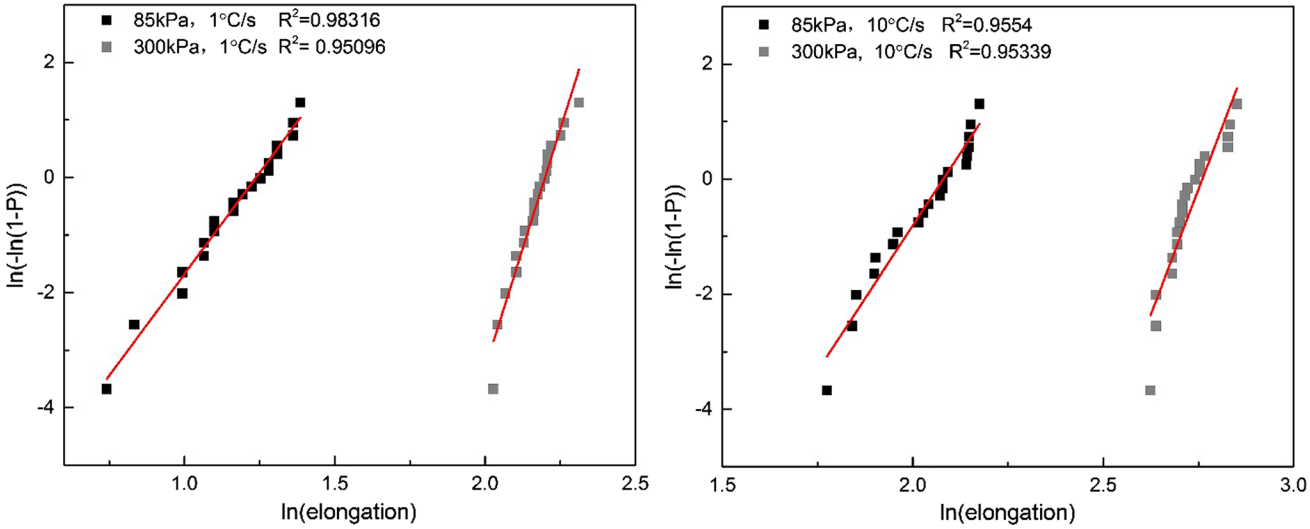

Fig. 10 Weibull plots of elongation data obtained from different experimental conditions

Table 5 Summary of the Weibull analysis

	UTS			Elongation		
Designation	**Value/MPa**	**Module**	R^2	**Value/%**	**Module**	R^2
LL	232	31.44	0.963	2.8	7.05	0.983
LH	267	47.53	0.910	9.1	10.09	0.955
HL	259	110.81	0.968	7.1	16.59	0.951
HH	293	123.9	0.916	13.5	17.39	0.953

Table 6 Analysis of variance for UTS

Source	**DF**	**SS**	***F* value**	***p* value**
Holding pressure	1	1190.25	4761	0.0092
Cooling rate	1	702.25	2809	0.012
Error	1	0.25	…	…

DF: The number of degrees of freedom from each source, *SS* the sum of squares
F value: The results of Fisher's test

Table 7 Analysis of variance for elongation

Source	**DF**	**SS**	***F* value**	***p* value**
Holding pressure	1	18.9225	7569	0.0073
Cooling rate	1	40.3225	16129	0.005
Error	1	0.0025	…	…

5. Conclusions

The effect of holding pressure on microstructure and mechanical properties of LPDC A356 aluminum alloy was investigated in detail in this research. Application of high holding pressure of 300 kPa was beneficial to refine the size of SDAS and eutectic silicon particles due to the faster cooling rate caused by high holding pressure. Meanwhile, the density was improved and the porosity defects content was decreased due to the better filling capability under high holding pressure. Tensile testing indicated that A356 aluminum alloy obtained under high holding pressure of 300 kPa and cooling rate of 10°C/s exhibited the highest tensile properties (UTS of 293 MPa and El% of 13.5%), improved by 9.7% in UTS and 48.4% in elongation, respectively, compared with the alloy obtained at the holding pressure of 85 kPa. In the experimental

condition of this study, the influence of variances on UTS and elongation can be significantly described by regression equations.

Acknowledgment

The authors gratefully acknowledge the financial support received from the National Key Research and Development Program of China (No. 2016YFB0300901).

References

1. W. Jiang, Z. Fan, D. Liu, D. Liao, X. Dong, and X. Zong, Correlation of Microstructure with Mechanical Properties and Fracture Behavior of A356-T6 Aluminum Alloy Fabricated by Expendable Pattern Shell Casting with Vacuum and Low-Pressure, Gravity Casting and Lost Foam Casting, *Mater. Sci. Eng., A*, 2013, **560**, p 396–403
2. C. Xu, F. Wang, H. Mudassar, C.Y. Wang, S.J. Hanada, W.L. Xiao, and C.L. Ma, Effect of Sc and Sr on the Eutectic Si Morphology and Tensile Properties of Al-Si-Mg Alloy, *J. Mater. Eng. Perform.*, 2017, **26**(4), p 1605–1613
3. H.C. Long, J.H. Chen, C.H. Liu, D.Z. Li, and Y.Y. Li, The Negative Effect of Solution Treatment on the Age Hardening of A356 Alloy, *Mater. Sci. Eng. A*, 2013, **566**, p 112–118
4. R. Chen, Y. Shi, Q. Xu, and B. Liu, Effect of Cooling Rate on Solidification Parameters and Microstructure of Al-7Si-0.3 Mg-0.15Fe Alloy, *Trans. Nonferrous Met. Soc. China*, 2014, **24**(24), p 1645–1652
5. A. Djebara, Y. Zedan, J. Kouam, and V. Songmene, *J. Mater. Eng. Perform.*, 2013, **22**(12), p 3840–3853
6. Z. Fan, Y. Wang, Y. Zhang, T. Qin, X.R. Zhou, G.E. Thompson, T. Pennycook, and T. Hashimoto, Grain Refining Mechanism in the Al/Al-Ti-B System, *Acta Mater.*, 2015, **84**, p 292–304
7. A. Razaghian, M. Emamy, A.A. Najimi, and S.H.S. Ebrahimi, Sr Effect on the Microstructure and Tensile Properties of A357 Aluminum Alloy and Al2O3/SiC-A357 Cast Composites, *Mater. Charact.*, 2009, **60**(11), p 1361–1369
8. Y. Tsai, S. Lee, and C. Lin, Effect of Trace Ce Addition on the Microstructures and Mechanical Properties of A356 (Al-7Si-0.35 Mg) Aluminum Alloys, *J. Alloys Compd.*, 2009, **35**(5), p 609–616
9. L. Bolzoni, M. Nowak, and N.H. Babu, Grain Refinement of Al-Si Alloys by Nb-B Inoculation. Part II: Application to Commercial Alloys, *Mater. Des.*, 2015, **66**, p 376–383
10. L. Bolzoni, M. Nowak, and N.H. Babu, Grain Refinement of Al-Si Alloys by Nb-B Inoculation. Part I: Concept Development and Effect on Binary Alloys, *Mater. Des.*, 2015, **66**, p 366–375
11. C. Xu, W. Xiao, R. Zheng, S. Hanada, H. Yamagata, and C. Ma, The Synergic Effects of Sc and Zr on the Microstructure and Mechanical Properties of Al-Si-Mg Alloy, *Mater. Des.*, 2015, **88**, p 485–492
12. J. Barbosa and H. Puga, Ultrasonic Melt Processing in the Low Pressure Investment Casting of Al Alloys, *J. Mater. Process. Technol.*, 2017, **244**, p 150–156
13. A. Jahangiri, S.P.H. Marashi, M. Mohammadaliha, and V. Ashofte, The Effect of Pressure and Pouring Temperature on the Porosity, Microstructure, Hardness and Yield Stress of AA2024 Aluminum Alloy During the Squeeze Casting Process, *J. Mater. Process. Technol.*, 2017, **245**, p 1–6
14. D. Dispinar, S. Akhtar, A. Nordmark, M.D. Sabatino, and L. Arnberg, Degassing, Hydrogen and Porosity Phenomena in A356, *Mater. Sci. Eng. A*, 2010, **527**(16), p 3719–3725
15. P. Zhang, Z. Li, B. Liu, and W. Ding, Effect of Chemical Compositions on Tensile Behaviors of High Pressure Die-Casting Alloys Al-10Si-yCu-xMn-zFe, *Mater. Sci. Eng. A*, 2016, **661**, p 198–210
16. G. Timelli, D. Caliari, and J. Rakhmonov, Influence of Process Parameters and Sr Addition on the Microstructure and Casting Defects of LPDC A356 Alloy for Engine Blocks, *J. Mater. Sci. Technol.*, 2016, **32**(6), p 515–523
17. H. Zhang, H. Zhang, Chinese patent: CN 105618710A, 20160601
18. G. Eisaabadi, B.P. Davami, S.K. Kim, N. Varahram, Y.O. Yoon, and G.Y. Yeom, Effect of Oxide Films, Inclusions and Fe on Reproducibility of Tensile Properties in Cast Al-Si-Mg Alloys: Statistical and Image Analysis, *Mater. Sci. Eng. A*, 2012, **558**, p 134–143
19. C.H. Catceres and B.I. Selling, Casting Defects and the Tensile Properties of an Al-Si-Mg Alloy, *Mater. Sci. Eng. A*, 1996, **220**(1), p 109–116
20. D.M. Stefanescu and A.V. Catalina, Physics of Microporosity Formation in Casting Alloys-Sensitivity Analysis for Al-Si Alloys, *Int. J. Cast Met. Res.*, 2011, **24**(3–4), p 144–150
21. W. Jiang, Z. Fan, D. Liao, D. Liu, Z. Zhao, and X. Dong, Investigation of Microstructures and Mechanical Properties of A356 Aluminum Alloy Produced by Expendable Pattern Shell Casting Process with Vacuum and Low Pressure, *Mater. Des.*, 2011, **32**(2), p 926–934